Title

Centrifuge modeling of temperature effects on the pullout capacity of torpedo piles in soft clay

Journal

Soils and Rocks, 45(1)

ISSN

1980-9743

Authors

Ghaaowd, Ismaail
McCartney, John
Saboya, Fernando

Publication Date

2022-03-09

DOI

10.28927/sr.2022.000822

Peer reviewed

Centrifuge modeling of temperature effects on the pullout capacity of torpedo piles in soft clay

Authors: Ismaail Ghaaowd, John S. McCartney[#] and Fernando Saboya

Author Information

Ismaail Ghaaowd, Ph.D.
Turner-Fairbank Highway Research Center (FHWA)
6300 Georgetown Pike, McLean, VA 22101, USA
Email: ismaail.ghaaowd.ctr@dot.gov

John S. McCartney, Ph.D., P.E., F.ASCE
Professor and Department Chair
Department of Structural Engineering
University of California San Diego
9500 Gilman Dr. La Jolla, CA 92093-0085
ORCID: 0000-0003-2109-0378
Email: mccartney@ucsd.edu

Fernando Saboya, Jr.
Professor
Department of Civil Engineering
State University of Norte Fluminense Darcy Ribeiro - UENF
Av. Alberto Lamego 2000 - CCT, Campos Rio 13 de Janeiro, Brazil, CEP 28016-812
Email: saboya@uenf.br

- Main text word count excluding the title page, notation list (e.g., symbols, abbreviations), captions of tables and figures, acknowledgments and references: 6987;
- Number of figures: 10;
- Number of tables: 3.

Abstract

This study presents the results from centrifuge modeling experiments performed to understand the effects of temperature changes on the vertical pullout capacity of scale-model torpedo piles embedded in soft clay layers. The model torpedo pile is a pointed stainless-steel cylinder with fins at the top, installed by self-weight to the base of a clay layer using a stepper motor. An internal electrical resistance heater was used to control the pile temperature. The torpedo pile was first heated until the temperature and pore water pressure of the surrounding clay layer stabilized (drained conditions), after which the torpedo pile was cooled. Pullout tests performed on torpedo piles indicate that allowing drainage of excess pore water pressures induced by heating to different temperatures followed by cooling leads to an increase in axial pullout capacity with maximum temperature but does not affect the pullout stiffness. Push-pull T-bar penetration tests performed before and after pile heating indicate that an increase in undrained shear strength of the clay occurs near the torpedo pile, and post-test gravimetric water content measurements indicate a greater decrease in void ratio occurred in the soil layers heated to higher temperatures. The pullout capacity of the torpedo pile was found to follow a linear trend with maximum pile temperature change, but with a smaller slope than that observed for end-bearing energy piles tested in previous studies in the same clay.

Keywords: Thermal improvement, torpedo piles, centrifuge physical modelling, pullout testing

List of symbols

A	Area
c_u	Undrained shear strength
D	Pullout displacement
e	Void ratio
H_w	Height of water above the surface of the clay layer
N	Centrifuge g-level
Q_{ult}	Pullout capacity
T_{pile}	Temperature of the pile
ΔF	Percent change in pile pullout capacity
ΔT	Change in temperature
ΔH	Change in soil layer height
Δu_w	Change in pore water pressure

1. Introduction

Torpedo piles are an economical method for anchoring offshore floating structures in deep water soil deposits (Bonfim dos Santos et al. 2006; Gilbert et al. 2008). Different sizes of torpedo piles are used in practice, with diameters varying from 0.75 to 1.10 m and lengths varying from 10 to 12 m. Larger torpedo piles are typically not encountered due to limitations in the capacities of transport vessels and offshore handling equipment. Although torpedo pile installation is cost effective as they are installed into the seafloor by self-weight penetration under high velocities associated with free fall through the water, the process of transporting the torpedo piles to a given location and rigging them for installation may be time consuming. Accordingly, any method to increase the pullout capacity of a torpedo pile so that the total number of piles required to anchor an offshore floating structure can be reduced will lead to significant cost savings. If the torpedo pile is embedded into clay layers in deep water conditions offshore, conventional soil improvement techniques like surcharge loading, vertical drains, electro-osmosis, are difficult to implement. Instead, thermal consolidation may be a useful approach for improvement of the soil surrounding the pile.

The concept of soil improvement using thermal consolidation is shown in Figure 1 for a torpedo pile installed within a clay layer. In this method, the torpedo pile is equipped with an internal heating element powered by either an electrical resistance heater or a chemical reaction. After installation, the heater can be operated to reach a target temperature or energy output. Depending on the drainage conditions of the soil, changes in pore water pressure Δu_w and soil surface settlement ΔH are expected for a given change in temperature ΔT. For undrained conditions, is well known that changes in temperature will lead to an increase in pore water pressure (Campanella and Mitchell 1968), with a magnitude depending on the plasticity index, initial void ratio, and initial effective stress (Ghaaowd et al. 2017). Further, heating of soils in undrained conditions will coincide with an initial thermo-elastic expansion (upward ΔH) of the soil around the pile (Uchaipichat and Khalili 2009). However, fully undrained conditions are not expected in the field for the boundary conditions shown in Figure 1. Instead, it is expected that the low permeability clay surrounding the heated torpedo pile will have partial drainage conditions, with some increase in pore water pressure during heating but less than that observed in fully undrained conditions. Regardless, the increase in pore water pressure in the clay next to the heated pile will lead to a hydraulic gradient. This hydraulic gradient will cause water to flow away from the pile and dissipation of the excess pore water pressure, a process referred to as thermal consolidation (Zeinali and Abdelaziz 2021). An increase then decrease in pore water pressure around a heating element in soft clay was observed in centrifuge modeling experiments by Maddocks and Savvidou (1984). It is important to maintain the elevated temperature during this water flow process, during which a permanent contraction of the soil is expected if the soil is normally consolidated or lightly overconsolidated (downward ΔH). The contraction of normally consolidated and lightly overconsolidated soils during drained heating has been observed in several element-scale studies (e.g., Baldi et al. 1988; Burghignoli et al. 2000; Cekerevac and Laloui 2004; Abuel-Naga et al. 2007a, 2007b; Towhata et al. 1993; Vega and McCartney 2015; Takai et al. 2016; Samarakoon and McCartney 2020). The coupling between changes in temperature and settlement have also been observed in the field. Bergenstahl et al. (1994) applied a change in temperature of approximately 60 °C to a 10 m-thick layer of clay over the course of 8.5 months and observed a thermally-induced settlement of 37 mm, while Pothiraksanon et al. (2010) applied a change in temperature of approximately 60 °C over the course of 200 days, and observed a thermally-induced settlement of approximately 120 mm. Cooling is expected to lead to a further contraction of the soil surrounding the pile, although contraction during cooling may depend on the rate of cooling. Thermal improvement is only appropriate for normally consolidated and lightly consolidated soils, as heavily overconsolidated soils are expected to expand and contract elastically during heating and cooling, respectively.

The in-situ heating-cooling process shown in Figure 1 is expected to lead to a reduction in void ratio e of the normally consolidated or lightly overconsolidated soil surrounding the torpedo pile. This is expected to lead to an increase in the average undrained shear strength of the soil layer along the length of the torpedo pile, which will in turn lead to an increase in the pullout capacity of the torpedo pile. The mechanisms of thermal improvement in the undrained shear strength of soft clay have been evaluated in element-scale tests in studies like Houston et al. (1985), Abuel-Naga et al. (2007c) and Samarakoon et al. (2018). These studies generally found that undrained shearing of soils after drained heating will lead to an increase in undrained shear strength. Houston et al. (1985) found that shearing of soils after undrained heating will lead to a decrease in undrained shear strength associated with the reduction in effective stress associated with the thermally induced pore water pressures. Accordingly, it is critical to ensure that the heating process is sufficiently long for the excess pore water pressures to dissipate. While most previous of the studies mentioned above focused on the increase in undrained shear strength due to heating alone, Samarakoon et al. (2018) found that a heating-cooling cycle leads to a further increase in shear strength of normally consolidated soil, and that the initial void ratio may play a role in the amount of change in shear strength of the soil. This observation is supported by the thermal consolidation experiments of Burghignoli et al. (2000) and Vega and McCartney (2015) who found that a heating-cooling cycle will lead to a further reduction in volume of soils than that encountered after heating alone.

There is evidence in the literature that thermal consolidation may be a useful technique to improve the pullout capacity of torpedo piles. Centrifuge modeling studies like Ghaaowd et al. (2018) and Ghaaowd and McCartney (2018, 2021) found that the pullout capacity of end-bearing piles embedded in soft clays could be improved by thermal consolidation induced by a heater embedded within the pile. The piles investigated in these previous studies extended through the full length of the clay layer, so thermal consolidation only affected the side shear resistance. Ng et al. (2014, 2021) performed centrifuge modeling studies on semi-floating energy piles in soft clay and observed settlement of the piles during cycles of heating and cooling, which can be attributed to thermal consolidation. However, they did not load the energy piles to failure after the heating-cooling cycles. Yazdani et al. (2019) performed pressure chamber tests to study the effects of elevated temperature on the shaft resistance of an energy pile in soft clay and observed an increased side shear capacity with increased temperature. Yazdani et al. (2021) attributed this increase to an increase in lateral earth pressure because the heating period in the experiments was not sufficient to permit full drainage of the pore water pressures. Different from the previous studies, torpedo piles are typically fully embedded within a soil layer, so heating may lead to an improvement in both the side shear capacity and the upward end bearing capacity. This justifies the need to perform further experiments on the effects of temperature on the pullout capacity of torpedo piles.

This study uses a centrifuge modeling approach developed by Ghaaowd et al. (2018) and Ghaaowd and McCartney (2021) to evaluate the effects of drained heating-cooling cycles on the pullout capacity of torpedo piles embedded in soft clay layers. Centrifuge modeling was used in this study because the pore water pressure generation during undrained heating is sensitive to the initial mean effective stress in the clay layer, and the effective stresses in a centrifuge model clay layer are similar to those in a prototype clay layer. Centrifuge modeling also permits the use of time scaling to simulate the effects of long duration heating-cooling cycles in the field, as diffusive time scales according to $1/N^2$ where N is the g-level (Ng et al. 2020). The Actidyne C61-3 centrifuge at the University of California San Diego was used to perform four tests on torpedo piles in separate clay layers. The four tests involved installation of self-weight installation of the torpedo pile into the clay layers at a constant displacement rate, heating to different target temperatures (20, 45, 65, and 80°C), cooling back to ambient temperature of 20 C, and vertical pullout of the torpedo pile at a constant displacement rate. In addition to presentation of the pullout versus displacement curves for the four tests, T-bar penetration results permit evaluation of the impact of the heating-cooling cycle on the undrained shear strength profiles of the clay layer near the torpedo piles.

2. Materials

The soil used in the centrifuge modeling experiments was kaolinite clay obtained from M&M Clays Inc. of McIntyre, Georgia. The liquid limit of the kaolinite clay is around 47% and the plastic limit was 28%, so the clay classifies as CL according to the Unified Soil Classification Scheme (USCS). An isotropic compression test performed by Ghaaowd and McCartney (2021) indicates that the slopes of the normal compression line (λ) and the recompression line (κ) for the clay are 0.080 and 0.016, respectively. The hydraulic conductivity of this kaolinite ranges from 2.8×10^{-9} to 8.2×10^{-9} m/s for void ratios ranging from 1.05 to 1.45, respectively. These values are relatively small indicating that partially drained conditions can be expected during heating of the torpedo pile as shown in Figure 1. Ghaaowd and McCartney (2021) reported that the thermal conductivity of this kaolinite ranged from 1.1 to 1.8 W/m°C for void ratios ranging from 3.0 to 0.8, respectively. Ottawa F-65 sand was used as a drainage layer at the base of the clay layers formed in this study. The grain size of this uniform sand varies from 0.1 mm to 0.5 mm, and the sand classifies as SP accordingly to the USCS. The hydraulic conductivity of the sand varies over a narrow range from 2.2×10^{-3} to 1.2×10^{-3} for the loosest and densest states, respectively (Bastidas 2016).

3. Experimental Setup

The centrifuge physical modeling tests were performed using a 50th-scale-model torpedo pile that fabricated from stainless steel, as shown in Figure 2(a). Although torpedo piles used in the field often have fins that extend the length of the main pile body for hydrodynamic stability (e.g., Bonfim dos Santos et al. 2004), the scale-model torpedo pile was designed to have a uniform cylindrical body with a sharp tip and fins only on the tail to simplify the heat transfer process from the main body of the torpedo pile by replicating a cylinder heat source. The main body of the scale-model torpedo pile has an outer diameter of 15.75 mm (0.79 m in prototype scale) and a length of 108.6 mm (5.43 m in prototype scale) and is hollow to accommodate a cylindrical heating element. The Firerod 1707 heating element from Watlow Electric Manufacturing, Inc. of St. Louis, MO has a length of 101 mm, a diameter of 12.6 mm, and fits snugly within the main cylindrical body of the torpedo pile. The heating element has a maximum power output of 500 W and was operated in temperature-control mode using feedback from an internal thermocouple connected to a Watlow temperature controller mounted on the centrifuge arm. The tip and the tail of the torpedo pile can be threaded into the main body of the torpedo pile to form the scale model torpedo pile having a total length of 160 mm (8 m in prototype scale). The tail of the torpedo pile incorporates a hole to pass the wires from the heating element and includes a horizontal hole that can be used to attach a cable for installation and pullout of the torpedo pile. The picture of the assembled scale-model torpedo pile is shown in Figure 2(b) after testing. The area for upward end bearing of the torpedo pile is complex due to the presence of the fins and the tapered tail section connected to the cabling, but it is clear from this picture that clay does interact with the tail. As will be discussed in the analysis section, an equivalent diameter of 15.75 mm equal to that of the main body of the torpedo pile was used to calculate the upward bearing capacity of the torpedo pile to account for these different bearing mechanisms.

A schematic of the container with an integrated loading system used to evaluate the effects of temperature effects on the pullout capacity of torpedo piles in clay is shown in Figure 3(a). The container consists of a cylindrical aluminum tank having an inner diameter of 550 mm, a wall thickness of 16 mm, and a height of 470 mm that resting atop an "O"-ring seal in a groove within a 620 mm-square base plate. The cylindrical tank is held down to the base plate via four hold-down tabs on the side of the cylinder that fit around 50-mm diameter threaded rods that are threaded into the 50 mm-thick base plate. A 620 mm-square upper reaction plate is mounted on the top of the threaded rods. The upper reaction plate supports stepper motors that are used for loading the torpedo pile (in the center of the container) and a T-bar penetrometer (offset from the center by 100 mm and not shown in Figure 3(a)) and serves as a mounting location for a 100 mm-long linear potentiometer used for tracking pullout displacement. The torpedo pile is connected via the stainless-steel cable to a load cell that is connected to the stepper motor in the center of the upper reaction plate, which permits the pile to be lowered into the clay layer under its self-weight and pulled out vertically after the thermal improvement process. Due to the length restrictions of the stepper motor drive rod within the centrifuge, the initial position of the T-bar was a depth of 60 mm (a prototype scale depth of 3 m) within the clay layer. Accordingly, the insertion and extraction of the T-bar only permitted characterization of the undrained shear strength profile from a depth of 60 mm to a depth of 220 mm (a prototype scale depth of 11 m) at a radial distance of 100 mm. Fortunately, the depth range of the T-bar penetration brackets the position of the torpedo pile prior to pullout. A picture of the container mounted in the centrifuge basket is shown in Figure 3(b) that shows the locations of the two stepper motors used for installation and extraction of the torpedo pile and T-bar along with the ports in the side of the container for installing sensors at different depths in the clay layer.

4. Experimental Procedures

The clay layer was prepared by mixing dry kaolinite clay in powder form with water under vacuum to form a slurry having a gravimetric water content of 130% (2.8LL). The slurry was carefully poured into the container to avoid air inclusions atop a 20 mm-thick layer of Ottawa sand that acts as a drainage layer. A filter paper and a 50 mm-thick porous stone having the same diameter as the inside of the cylinder were placed atop the clay layer. After 24 hours of self-weight consolidation, dead-weights corresponding to vertical stresses of 2.4, 6.3, and 10.2 kPa were added atop the porous stone in 24-hour increments. The first dead weight included an aluminum disk that helped to distribute the vertical stress of the dead weights atop the porous stone. The vertical stress was then increased to 23.6 kPa using a hydraulic piston that reacted against the upper reaction plate, which was maintained for another 24 hours. After this time, the upper reaction plate was removed, and the hydraulic piston was replaced with the stepper motor assemblies for the foundation and the T-bar. After the 1g consolidation of the clay layers was completed, six type K thermocouples and five miniature Druck PDCR 81 pore water pressure sensors were inserted through the container side wall into the clay layer. The sensor insertion was facilitated by attaching the sensor cable to a thin rod as summarized by Ghaaowd and McCartney (2021). After processing the data from the experiments, it was found that only two of the pore water pressure sensors gave meaningful results (PPT3 and PPT4) and the other pore water pressure sensors had been damaged in an early experiment. Because the positions of the sensors may change after consolidation in the centrifuge, the final positions of the sensors were verified at the end of the experiment when excavating the clay layer, as summarized in Table 1. Because the sensor locations were slightly different in each experiment as noted in Table 1, the sensors locations are not shown in Figure 3.

The assembled container was then placed inside the centrifuge basket for in-flight self-weight consolidation at 50 g. This procedure was found to produce a normally-consolidated clay layer with an overconsolidated portion near the surface. More details of the soil layer preparation are provided in Ghaaowd and McCartney (2021). During in-flight self-weight consolidation at 50 g, the excess pore-water pressures were monitored using the pore pressure transducers. A typical time series of the pore water pressure during centrifugation was presented in Ghaaowd and McCartney (2021) for a test on an end-bearing energy pile test that confirms that the clay layer reached more than 90% of primary consolidation before moving to the next testing stage. The void ratio at the end of self-weight consolidation in the four different tests was approximately 1.4, while after self-weight consolidation a decrease in void ratio with depth was observed in post-test measurements as will be reported later in the paper. The clay layer thickness in the four experiments after 1 g consolidation was approximately 235 mm (11.75 mm in prototype scale), and a thin layer of water was permitted atop the clay layer ranging from H_w = 40 to 70 mm. This water layer was connected via a standpipe to a drain at the bottom of the container, so the clay layer was effectively double drained during the duration of the experiment.

After stabilization at 50 g, the torpedo pile was installed in flight into the sedimented clay layers. Although torpedo piles are typically installed in the field by being dropped through water from a certain depth so that it penetrates at high velocity to a target depth, it was not possible to simulate this high velocity installation approach in the centrifuge. To lead to repeatability between the different experiments and to ensure the verticality of the torpedo pile after installation, the torpedo piles in this study were installed by lowering them under their self-weight into the soft clay using the cable connected to the stepper motor at a model-scale velocity of 0.1 mm/s. While this is a much slower velocity than torpedo piles may experience in the field, it is sufficient to lead to undrained conditions. Using this approach, the pile tip was able to pass through the clay layer and become embedded in the dense sand layer. This penetration depth was confirmed by the position of the stepper motor, and by the fact that the load cell connected to the torpedo pile cable indicated no load and the mooring cable went slack. The torpedo pile was inserted so that the height of clay above the torpedo pile is approximately 94 mm (4.7 m in prototype scale). When the excess pore water pressure generated due to the pile insertion dissipated, the temperature of the heated torpedo pile was increased using the Watlow heat controller until reaching the target temperature at the pile wall. As mentioned, it was important for heating to continue during centrifugation until the soil temperature and pore water pressure stabilized, which typically required 5-10 hours in model scale (520 to 1040 days in prototype scale). However, for consistency in comparison of results all the tests on heated piles involved heating for approximately 30 hours in model scale, which was longer than necessary for thermo-hydraulic equilibrium and corresponds to a total duration of heating in prototype scale is 3125 days or 8.56 years. After this point, the pile was cooled for 10 hours in model scale and was then pulled out at the same velocity as used for installation.

After pullout testing of the pile the T-bar penetrometer, with a T diameter of 14 mm, a T length of 57 mm, and a shaft diameter of 11 mm, was used to measure the undrained shear strength profiles of the clay layers containing the heated and unheated torpedo piles. Insertion of the T-bar into the clay layer can be used to infer the undrained shear strength of the intact clay layer as a function of depth, while extraction of the T-bar can be used to infer the undrained shear strength of disturbed clay as a function of depth (Stewart and Randolph 1994). As mentioned, the T-bar was designed to permit model-scale penetrations between 60 and 235 mm and was driven by a second stepper motor at a model-scale velocity of 0.2 mm/s to ensure undrained conditions during insertion and extraction. T-bar penetration tests were performed after pile pullout testing in each clay layer at a radius of 100 mm from the heated and unheated torpedo piles (6.35 pile diameters), which is far enough away to be undisturbed from the pile insertion and extraction based on the pore water pressure measurements, but close enough to be influenced by temperature based on the thermocouple measurements.

5. Results

5.1 Thermo-Hydraulic Response of the Pile and Clay Layer

Model-scale time histories of temperature at different locations in the four tests are shown in Figure 4. The maximum pile temperatures and maximum changes in pile temperature summarized in Table 2. There were generally 5 stages in each of the tests which are delineated in the figures using vertical dashed lines, including: (I) consolidation of the clay layer during centrifugation; (II) insertion of the torpedo pile under self-weight; (III) heating of the pile and surrounding soil; (IV) cooling of the pile and surrounding soil; and (V) pullout of the pile. In all the tests, there was a slight cooling effect as the centrifuge spun up followed by a slight warming due to centrifuge operation. The average surface temperature of 20 °C in the baseline Test T1 shown in Figure 4(a) was used as a reference temperature when calculating the changes in pile temperature. In the tests on heated torpedo piles in Tests T2, T3, and T4, the pile temperature rapidly increased to the target temperatures of 45, 65, and 80 °C, and approximately 5-10 hours was required for the temperatures at the different monitoring points in the clay layer to stabilize. After the approximately 30 hours of heating in each of the tests, cooling back to ambient conditions was achieved in approximately 5 hours even though 10 hours was permitted.

Profiles of temperature with radial location at steady-state conditions, which was selected as a time of 25 hours after the start of heating in Stage (III) are shown in Figure 5. Two observations from these profiles are that the temperature of the clay was nonlinearly distributed with radial location, and that the clay even at locations relatively close to the pile did not approach the temperature of the torpedo pile. In Test T2 the closest thermocouple was 26 mm away from the torpedo pile, while in Tests T3 and T4 there were two thermocouples closer to the pile that indicated a sharp drop-off in temperature. Accordingly, it is likely that a similar sharp drop-off in temperature occurred in the clay near the torpedo pile in Test T2. It is interesting that even when applying a pile temperature of 80 °C (change in pile temperature of 60 °C) that the clay temperature at a model-scale radial location of 11 mm (3.125 mm from the pile) only experienced a change in temperature of 35 °C. This is partly due to the high thermal conductivity of the stainless-steel torpedo pile, which likely permitted upward and downward heat transfer in addition to lateral heat transfer. The implication of this sharp drop-off in the radial temperature distribution around the cylindrical heat source is that the magnitude of the change in pore water pressure in the clay may be smaller than that associated with the full change in pile temperature. While changes in temperature of the clay were observed out to a prototype-scale radial location of more than 7 m (a model-scale radial location 150 mm) or nearly9.5 pile diameters, the largest changes in temperature were within 2 pile diameters of the torpedo pile. This indicates that the greatest thermal improvement of the clay layer will occur relatively close to the torpedo pile.

Model-scale time series of pore water pressure at two locations in the clay layers are shown in Figure 6. The magnitudes of pore water pressure depend on the ponded water height and the actual locations of the pore water pressure sensors as measured at the end of the tests. A decrease in pore water pressure is observed in Stage (I) while the clay layer consolidates in the centrifuge, and a small increase in pore water pressure occurs when the pile is inserted into the clay layer in Stage (II). Some additional consolidation of the clay layer likely occurred in Stage (II) during pile insertion, but this study is not focused on the penetration resistance of the torpedo pile during insertion. During heating in Stage (III), only a very small increase in pore water pressure was observed. During cooling in Stage (IV) a small decrease in pore water pressure was observed, but of a smaller magnitude than that observed during heating. During pullout in Stage (V) a large increase in pore water pressure was observed.

The pore water pressure response during heating is better highlighted in the excess pore water pressure versus the time of heating (model scale) in Figure 7. The maximum increases in pore water pressure in Tests T2, T3, and T4 were 1.5, 2.0, and 2.0 kPa, respectively. The similar excess pore water pressures in Tests T3 and T4 could be explained by the closer location of PPT3 in Test T3 and the similar changes in temperature of the pile at the radial locations of these sensors as shown in the change in temperature profiles in Figure 5. The excess pore water pressures all show a rapid generation followed by dissipation within approximately 5 hours of heating time. The thermal improvement process closer to the pile may have taken a longer duration, which was the reason for the longer model-scale heating duration of 30 hours in the centrifuge tests. Similar to the excess pore water pressure results presented in Ghaaowd and McCartney (2021) for end-bearing energy piles in clay, the magnitudes of excess pore water pressure were less than those obtained using the undrained thermal pressurization model of Ghaaowd et al. (2017), likely due to partial drainage in the centrifuge experiments.

5.2 Torpedo Pile Pullout Response

The prototype-scale pullout load versus displacement curves for the heated and unheated torpedo piles in clay layers having similar initial conditions are shown in Figure 8(a). All four pullout curves start from a self-weight load of 122 kN. An increase in pullout capacity with the increase in maximum pile temperature is observed. The maximum pullout force versus the maximum pile temperature is shown in Figure 8(b). A linear trend is observed in this figure, indicating that higher pile temperatures will lead to greater thermal improvement. The difference in pullout capacity for the piles with maximum temperatures of 20 and 80 °C was 56 kN in prototype scale, which corresponds to a relative difference of 58% percent. This is a substantial increase in pullout capacity that indicates that thermal improvement was successful.

The stiffness of the pullout curves in Figure 8(a) is relatively similar for all four tests, which is a similar observation that that made by Ghaaowd and McCartney (2021) when analyzing tests on end-bearing energy piles in soft clay. It was expected that the increase in undrained shear strength of the clay layer with thermal improvement would also correspond to an increase in stiffness of the clay-pile interface. The similar stiffnesses observed in Figure 8(b) may have occurred because the heated torpedo piles experienced thermal axial strains in the direction opposite to gravity during heating that may have counteracted the positive effect of the thermal improvement in the stiffness. Further research is needed to understand the effects of thermal improvement on the stiffness response during torpedo pile pullout, but it is clear from these tests that thermal improvement has a positive effect on the magnitude of pullout capacity.

5.3 T-bar Penetration Test Results

The T-bar penetration results for the clay layers with unheated and heated torpedo piles permit evaluation of the effects of cyclic heating-cooling to different temperatures from an initial temperature of 20 °C on the behavior of normally consolidated clay layers. The undrained shear strength profiles for the clay layer at a model-scale distance of 100 mm from the four torpedo piles are shown in Figure 9(a). The correlations of Stewart & Randolph (1991) were used to interpret the undrained shear strength profiles from the T-bar penetration results. A problem with the stepper motor in Test T3 prevented a T-bar test from being performed after the pile was heated to 65 °C, but from the other three tests the T-bar tests indicate an increase in undrained shear strength in the middle section of the clay layer with increasing maximum pile temperature. The changes in clay temperature at a model-scale radial location of 100 mm (a prototype-scale radial location of 5 m) are much smaller than those of the pile as shown in Figure 5, but a clear improvement is still observed at this location. The positive undrained shear strengths during insertion of the T-bar were generally greater than the negative undrained shear strength during extraction of the T-bar, but a typical bell-shaped curve was noted in all three tests. The thickness of the sand layer may have been slightly greater in Test T1 which explains the large increase in undrained shear strength at the bottom of the clay layer. The maximum, minimum, and average undrained shear strengths along the length of the torpedo pile obtained from the profiles in Figure 9(a) are summarized in the last column of Table 2.

At the end of testing, soil samples were obtained at the radial location of the T-bar on the opposite side of the profile. Samples were not obtained from near the center of the profile due as they may not be representative of the conditions after heating due to the disturbance caused by pullout of the torpedo pile. The void ratios inferred from gravimetric water content samples at the end of the tests are shown in Figure 9(b). Lower void ratios are observed in the clay layers that experienced higher temperatures, which correspond well with the increases in the undrained shear strength with temperature inferred from the T-bar penetration tests. While the results from the T-bar and soil samples after testing cannot be directly correlated with the pullout tests due to the differences in the locations of these measurements, they are good indicators that thermal improvement occurred in the clay layer due to torpedo pile heating.

6. Analysis and Comparison with End Bearing Energy Pile Pullout

The pullout capacity of torpedo piles Q_{ult} can be estimated using the following equation used by Gilbert et al. (2004) for the pullout of torpedo piles:

$$Q_{ult} = Q_{side} + Q_{end} = \alpha c_{u,average} A_{side} + c_{u,end} N_c d_c s_c A_{end} \quad (1)$$

where Q_{side} is the side shear capacity, Q_{end} is the upward end bearing capacity, α is a side shear reduction factor to account for installation effects, $c_{u,average}$ is the average undrained shear strength along the length of the torpedo pile, A_{side} is the area of the sides of the torpedo pile in clay, $c_{u,end}$ is the undrained shear strength at the upper end of the torpedo pile, $N_c d_c s_c$ is the adjusted undrained bearing capacity factor for a deep foundation equal to 9, and A_{end} is the equivalent cross-sectional area of the end of the torpedo pile to account for the taper and presence of the fins as shown in Figure 2(a). Specifically, the value of A_{end} was assumed to be equal to the cross-sectional area of the main body of the torpedo pile for simplicity. The upward end bearing capacity was calculated for each of the piles using the minimum undrained shear strength values from the T-bar tests in Table 2 (which correspond to the level of the upper end of the torpedo pile). The undrained shear strength at the level of the upper end of the pile for Test T3 was assumed to be linearly distributed between values measured at that level in Tests T2 and T3. The calculated upward end bearing capacities are summarized in Table 3, along with the side shear capacities calculated as the difference between the measured ultimate pullout capacity and the calculated upward end bearing capacities. Using the calculated side shear capacity for the torpedo pile tested at room temperature conditions, the average undrained shear strength from the T-bar test in Table 2 (which was assumed to be the same as at the soil-pile interface), and the side area of the pile, a value of α was back-calculated to be 0.4, which represents both a lower interface shear strength than the undrained shear strength of the soil and the effects of installation on the interface shear strength. Gilbert et al. (2004) assumed $\alpha = 1$, and found a consistent overprediction of the pullout capacity indicating that a lower value of α like that used in this study may be appropriate. This same value of α was then used to back-calculate the average undrained shear strength values at the soil-pile interface for each of the tests on the heated torpedo piles, which are summarized in the last column of Table 3. An increase in average undrained shear strength at the soil-pile interface occurred with the increase in maximum pile temperature. The magnitudes are greater than the undrained shear strength values from the T-bar tests measured at a prototype-scale distance of 5 m from the pile and represent the undrained shear strength at the clay-pile interface. While this analysis is simple and could be improved through further testing of physical models, it is helpful to understand the different ways that thermal improvement can enhance the pullout capacity of torpedo piles.

A comparison of the percent increase in pullout capacity of the torpedo pile in soft clay with the maximum change in temperature during heating with similar values measured from centrifuge tests on end-bearing energy piles in the same clay layer in centrifuge tests performed by Ghaaowd and McCartney (2018, 2021) is shown in Figure 10. A linear trend is observed for the torpedo piles and the end-bearing energy piles, but the slope of the trend line is steeper for the end-bearing energy piles. The end-bearing energy piles extended through the full length of the clay layer having a similar thickness to the clay layer investigated in this study, so a greater length of clay was improved. In their experiments, thermal improvement only affected the side shear capacity of the piles as the top of the end-bearing energy piles was extending out of the clay layer. Overall, this comparison confirms the feasibility of thermal improvement of the pullout capacity of piles from soft clay in general and emphasizes the importance of the configuration of the energy pile in the clay subsurface when estimating increases in pullout capacity.

7. Conclusions

Torpedo piles in soft clay layers were evaluated at a scale of 1/50 in a geotechnical centrifuge to evaluate the impacts of a pile heating-cooling cycle on the behavior of the clay layer and the corresponding pullout capacity of the torpedo pile. Measurements of temperature and pore water pressure in the clay layer surrounding the piles supports the hypothesis that thermal consolidation leads to the improvement in shear strength. These measurements also indicate that the zone of influence of the change in temperature is primarily within 2 pile diameters from the heated torpedo pile and that the thermal consolidation process is mostly complete after 500 days in prototype scale (a model-scale time of 5 hours). The undrained shear strength values of the clay layers surrounding the heated-cooled torpedo piles inferred from T-bar penetration tests and from the pile pullout tests were found to be greater than that of a clay layer surrounding an unheated torpedo pile. A reduction in void ratio was also observed at the end of testing for clay layers that had experienced higher temperatures. The pullout capacities of the torpedo piles that had experienced greater changes in temperature during the heating-cooling cycle were greater than that of the unheated torpedo pile. The slopes of the pullout load versus displacement curves were similar, which may be due to the impact of upward displacements associated with thermal expansion of the heated torpedo piles prior to pullout, leading to an initially elastic pullout response for all the torpedo piles. The amount of the improvement in the torpedo pile capacity was found to increase linearly with the maximum change in temperature of the pile, but with a lower slope than that measured for tests on end-bearing energy piles in the same soft clay in previous studies.

Acknowledgements

Support from the University of California San Diego is appreciated. The views in this paper are those of the authors alone.

Declaration of Interests

The authors have no conflicts of interest.

References

Abuel-Naga, H. M., Bergado, D. T., Bouazza, A. and Ramana, G.V. (2007a). “Volume change behavior of saturated clays under drained heating conditions: experimental results and constitutive modeling.” Canadian Geotechnical Journal. 44(8), 942-956.

Abuel-Naga, H.M., Bergado, D.T., Bouazza, A. (2007b). “Thermally induced volume change and excess pore water pressure of soft Bangkok clay.” Engineering Geology. 89, 144-154.

Abuel-Naga, H. M., Bergado, D. T., Lim, B.F. (2007c). “Effect of temperature on shear strength and yielding behavior of soft Bangkok clay.” Soils and Foundations. 47(3), 423-436.

Baldi, G., Hueckel, T., Pellegrini, R. (1988). “Thermal volume changes of the mineral-water system in low-porosity clay soils.” Canadian Geotechnical Journal. 25(4), 807-825.

Bastidas, A.M. (2016). “Ottawa F-65 Sand Characterization.” Ph. D. Dissertation, University of California, Davis.

Bergenstahl, L., Gabrielsson, A., Mulabdic, M., (1994). "Changes in soft clay caused by increases in temperature." Proc. 13th Int. Conf. on Soil Mech. and Found. Eng., New Delhi, pp. 1637–1641.

Bonfim dos Santos, A., Henriques, C.C.D., and Pimenta, J.M.H.A. (2004). "Improvements achieved in the project of FPSO P-50." Offshore Technology Conference, Houston, May, 2004, Paper No. OTC 16705.

Burghignoli, A., Desideri, A., and Miliziano, S. (2000). "A laboratory study on the thermomechanical behavior of clayey soils." Canadian Geotechnical Journal. 37(4), 764-780.

Campanella, R.G., and Mitchell, J.K. (1968). "Influence of temperature variations on soil behavior." Journal of the Soil Mechanics and Foundation Division, 94(SM3), 709-734.

Cekerevac, C., and Laloui, L. (2004). Experimental study of thermal effects on the mechanical behaviour of a clay. International Journal for Numerical and Analytical Methods in Geomechanics. 28, 209–228.

Dennis, N.D., and Olson, R.E. (1983). "Axial capacity of steel pipe piles in clay." Proc., Conf. on Geotech. Pract. In Offshore Eng., S. G. Wright, ed., ASCE, New York: 370–388.

Ghaaowd, I. and McCartney, J.S. (2018). "Centrifuge modeling of temperature effects on the pullout capacity of energy piles in clay." DFI 43rd Annual Conference on Deep Foundations. Anaheim, CA. Oct 24-27. 1-7.

Ghaaowd, I. and McCartney, J.S. (2021). "Centrifuge modeling methodology for energy pile pullout from saturated soft clay." ASTM Geotechnical Testing Journal. DOI: 10.1520/GTJ20210062.

Ghaaowd, I., Takai, A., Katsumi, T., McCartney, J.S. (2017). "Pore water pressure prediction for undrained heating of soils." Environmental Geotechnics. 4(2): 70-78.

Ghaaowd, I., McCartney, J.S., Huang, X., Saboya, F., and Tibana, S. (2018). "Issues with centrifuge modeling of energy piles in soft clays." Proceedings of the 9th International Conference on Physical Modeling in Geotechnics: Physical Modelling in Geotechnics. A. McNamara et al., eds. Taylor & Francis Group, London. 1365-1370.

Gilbert, R.B., Morvant, M., and Audibert, J. (2008). Torpedo Piles Joint Industry Project - Model Torpedo Pile Tests in Kaolinite Test Beds. Report to Minerals Management Service. University of Texas. Austin. 48 pg.

MarchHouston, S.L., Houston, W.N., and Williams, N.D. (1985). "Thermo-mechanical behavior of seafloor sediments." Journal of Geotechnical Engineering. 111(12), 1249-1263.

Hueckel, T., Pellegrini, R. and Del Omo, C. (1998). “A constitutive study of thermo-elastoplasticity of deep carbonatic clays.” International Journal of Numerical and Analytical Methods in Geomechanics, Vol. 22, No. 7, pp.549-574.

Maddocks, D.V. and Savvidou, C. (1984). “The effect of the heat transfer from a hot penetrator installed in the ocean bed.” Proc. Symp. On the Application of Centrifuge Modeling to Geotechnical Design. W.H. Craig. Manchester U.K

McCartney, J.S. and Murphy, K.D. (2017). “Investigation of potential dragdown/uplift effects on energy piles.” Geomechanics for Energy and the Environment. 10(June): 21-28.

Ng, C.W.W., Shi, C., Gunawan, A., and Laloui, L. (2014). “Centrifuge modelling of energy piles subjected to heating and cooling cycles in clay.” Géotech. Lett. 4(4), 310–316.

Ng, C.W.W., Farivar, A., Gomaa, S.M.M.H., and Jafarzadeh, F. (2021). “Centrifuge modeling of cyclic nonsymmetrical thermally loaded energy pile groups in clay. Journal of Geotechnical and Geoenvironmental Engineering. 147(2), 04021146.

Ng, C.W.W., Zhang, C., Farivar, A., and Gomaa, S.M.M.H. (2020). “Scaling effects on the centrifuge modelling of energy piles in saturated sand.” Géotechnique Letters. 10(1), 57-62.

Pothiraksanon, C., Bergado, D.T. and Abuel-Naga, H.M. (2010). “Full-scale embankment consolidation test using prefabricated vertical thermal drains.” Soils and Foundations, 50(5): 599-608.

Samarakoon, R., Ghaaowd, I. and McCartney, J.S. (2018). “Impact of drained heating and cooling on undrained shear strength of normally consolidated clay.” International Symposium on Energy Geotechnical SEG-2018, Switzerland. 243-250.

Samarakoon, R., and McCartney, J.S. (2020). “Role of initial effective stress on the thermal consolidation of normally consolidated clays.” Proc. 2nd International Conference on Energy Geotechnics (ICEGT-2020). E3S Web of Conferences, Les Ulis, France. 205, 09001. https://doi.org/10.1051/e3sconf/202020509001.

Stewart, D. and Randolph, M. (1994). “T-Bar penetration testing in soft clay.” Journal of the Geotechnical Engineering Division. ASCE. 120(12): 2230-2235.

Takai, A., Ghaaowd, I., Katsumi, T., and McCartney, J.S. (2016). “Impact of drainage conditions on the thermal volume change of soft clay.” GeoChicago 2016: Sustainability, Energy and the Geoenvironment. Chicago. Aug. 14-18. pp. 32-41.

Towhata, I., Kuntiwattanakul, P., Seko, I., and Ohishi, K. (1993). “Volume change of clays induced by heating as observed in consolidation tests.” Soils and Foundations. 33(4), 170-183.

Uchaipichat, A. Khalili, N. “Experimental investigation of thermo-hydro-mechanical behaviour of an unsaturated silt.” Géotechnique. 59(4), (2009), 339–353.

Vega, A. and McCartney, J.S. (2015). “Cyclic heating effects on thermal volume change of silt.” Environmental Geotechnics. 2(5), 257-268.

Yazdani S., Helwany S., and Olgun G. (2019). “Investigation of thermal loading effects on shaft resistance of energy pile using laboratory-scale model.” Journal of Geotechnical and Geoenvironmental Engineering, 145(9): 04019043.

Yazdani S., Helwany S., and Olgun G. (2021). “The mechanisms underlying long-term shaft resistance enhancement of energy piles in clays.” Canadian Geotechnical Journal. 58, 1640-1653.

Zeinali, S.M. and Abdelaziz, S.L. (2021). “Thermal consolidation theory.” Journal of Geotechnical and Geoenvironmental Engineering. 147(1), 04020147.

TABLE 1: Sensor locations in the four tests

Sensor	Test T1		Test T2		Test T3		Test T4	
	r mm	Depth mm	r mm	Depth mm	r mm	Depth mm	r mm	Depth mm
TC1	Surface		26	225	16	240	11	225
TC3	-	-	36	190	21	205	22	190
TC4	-	-	56	145	26	160	46	145
TC2	-	-	61	160	46	175	31	160
TC5	-	-	91	165	86	180	78	165
TC6	-	-	141	180	135	195	121	180
PPT3	140	36	51	170	46	180	66	180
PPT4	140	36	66	220	66	190	66	160

TABLE 2. Summary of tests on the torpedo piles after a heating-cooling cycle involving different maximum pile temperatures during centrifugation at N=50g

Test	Pile Temperature during Heating °C	Change in Pile Temperature °C	Maximum Pullout Load (Prototype Scale) kN	Percent Improvement in Pile Pullout Capacity %	Min/Ave./Max. Undrained Shear Strength from T-bar* (kPa)
T1	20	0	-97	-	7.2/12.7/18.2
T2	45	25	-117	19	10.6/14.4/18.2
T3	65	45	-139	42	-
T4	80	60	-153	56	11.6/15.3/19.0

* Defined over the length of the torpedo pile at a radius of 5 m or a distance of 4.6 m from the edge of the torpedo pile (prototype scale)

TABLE 3. Analysis of torpedo pile capacity components (prototype scale)

Test	Maximum Pullout Load kN	Calculated Upward End Bearing Capacity[1] kN	Calculated Side Shear Capacity kN	Back-Calculated Average Undrained Shear Strength at Pile-Clay Interface[2] kPa
T1	-97	-31	-66	12.2
T2	-117	-46	-71	13.1
T3	-139	-48	-90	16.7
T4	-153	-51	-102	19.0

[1] Calculated assuming an end area corresponding to a circular area corresponding to the fins.
[2] Calculated assuming a reduction factor of $\alpha = 0.4$

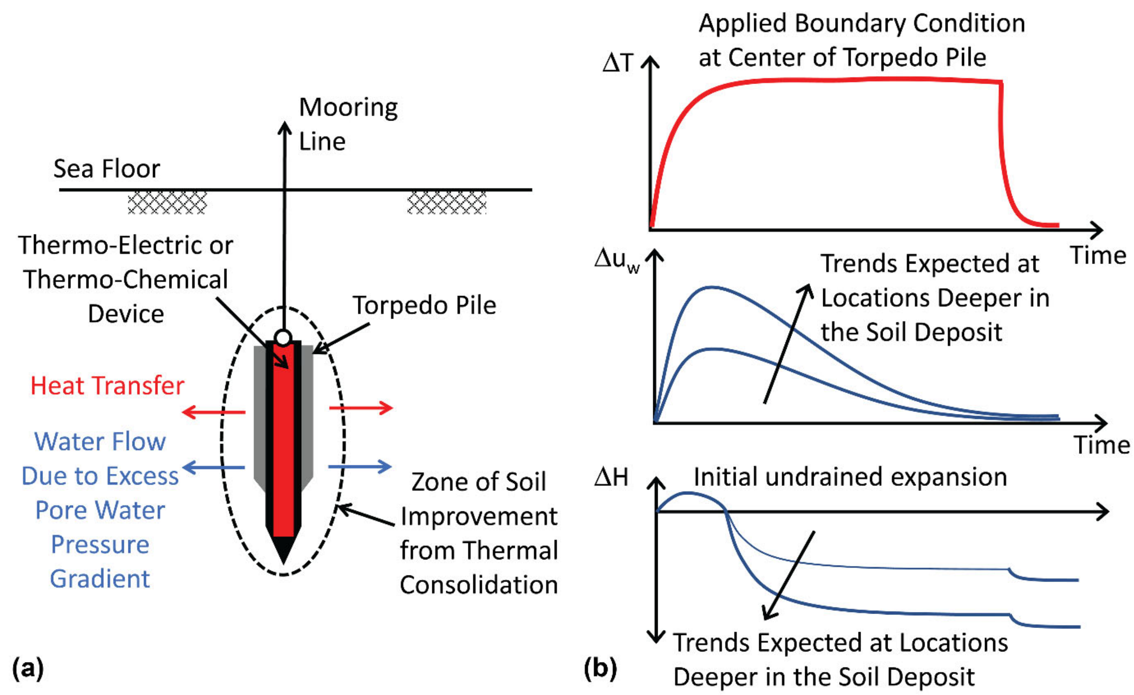

FIG. 1. Concept of thermal improvement of soft clays around torpedo piles: (a) Schematic of an installed torpedo pile with an internal heater; (b) Hypothetical trends in pile temperature, excess pore water pressure in soil at different depths, and changes in soil volume surrounding the torpedo pile

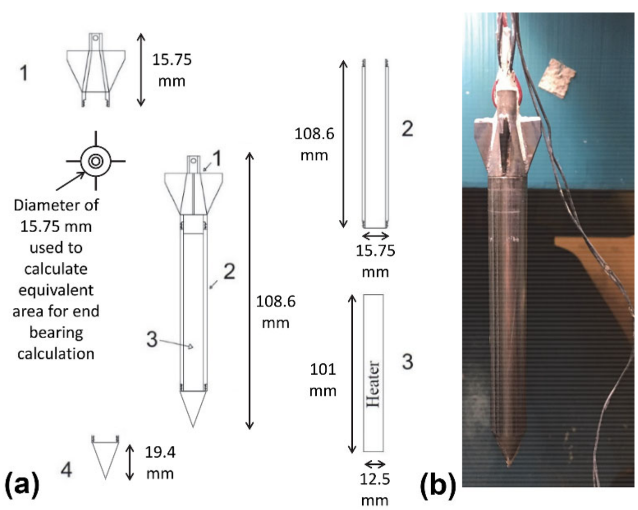

FIG. 2. Centrifuge-scale torpedo pile (a): Schematic showing: (1) Top cap with fins, (2) Body, (3) Internal electric resistance heater, (4) Pointed tip; (b) Picture showing mooring line connection to the top cap of the torpedo pile

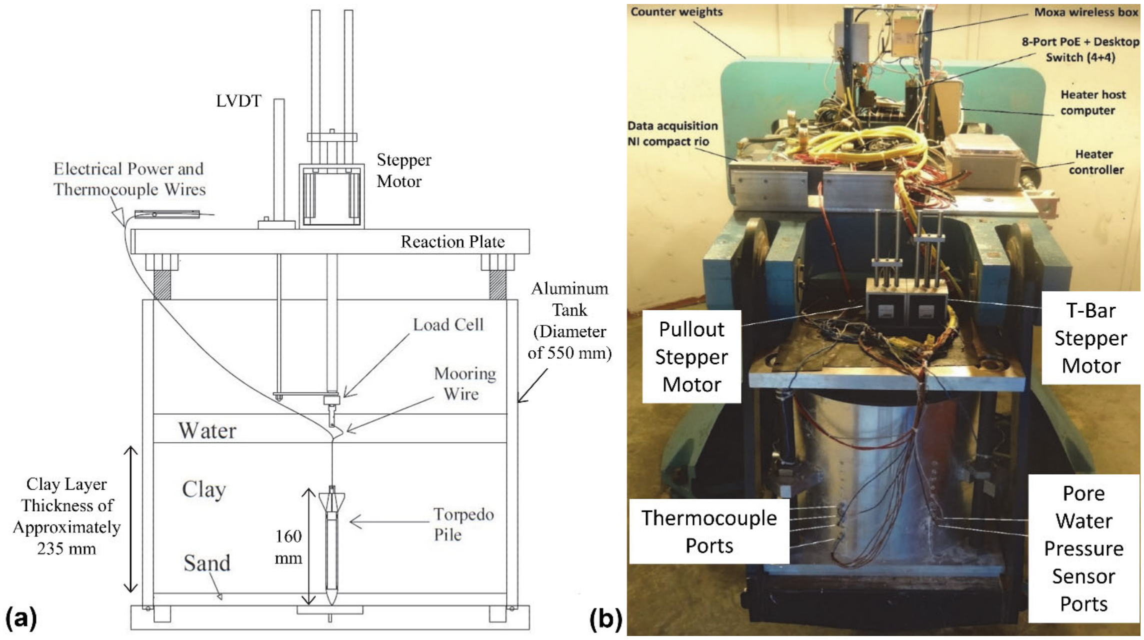

FIG. 3. Experimental setup: (a) Cross-sectional schematic of the setup showing the installed torpedo pile location; (b) Picture of the setup mounted on the centrifuge basket

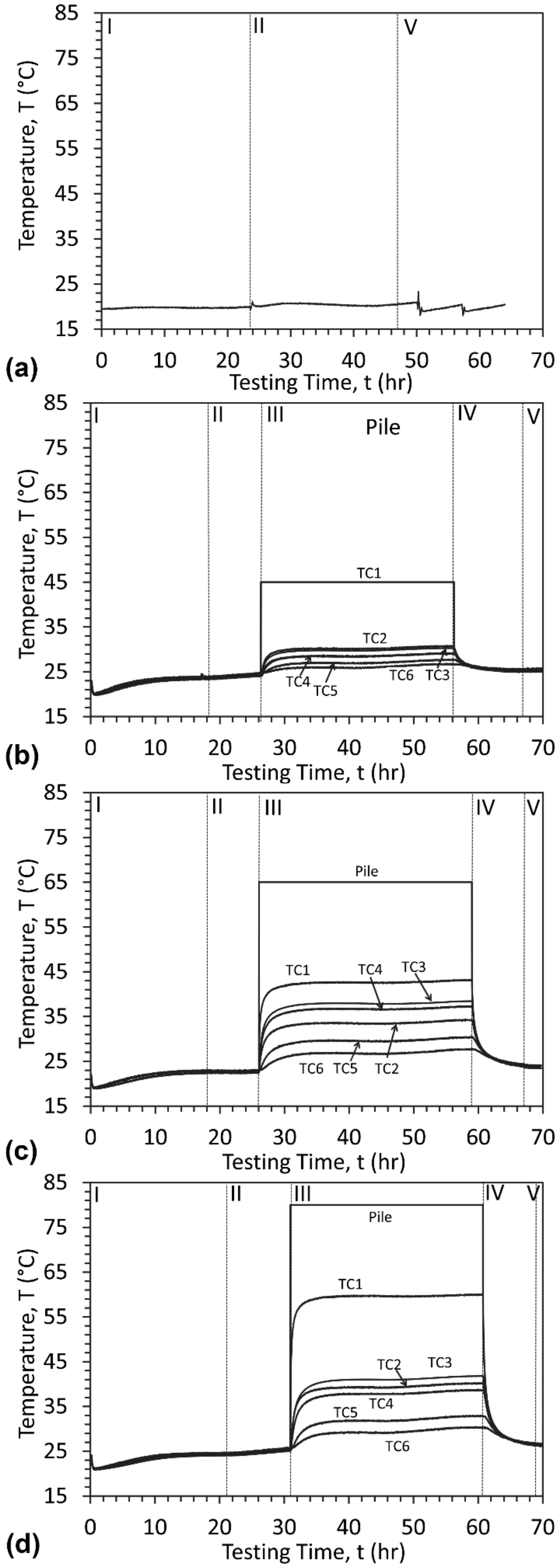

FIG. 4. Time series of temperature readings at different radii from the torpedo pile during the five testing stages: (a) Test T1 (clay surface only); (b) Test T2; (c) Test T3; (d) Test T4

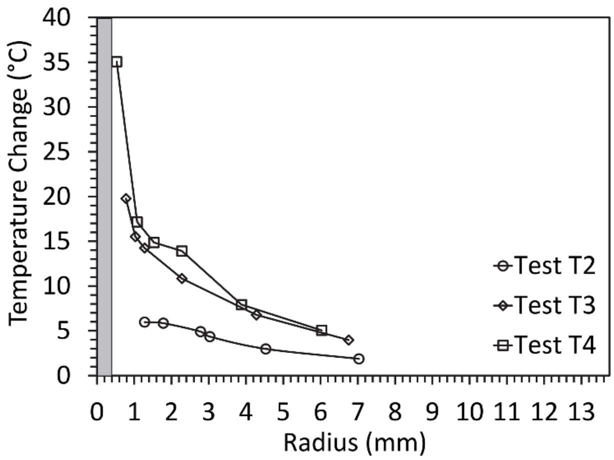

FIG. 5. Prototype-scale equilibrium temperature profiles in the three tests on heated torpedo piles

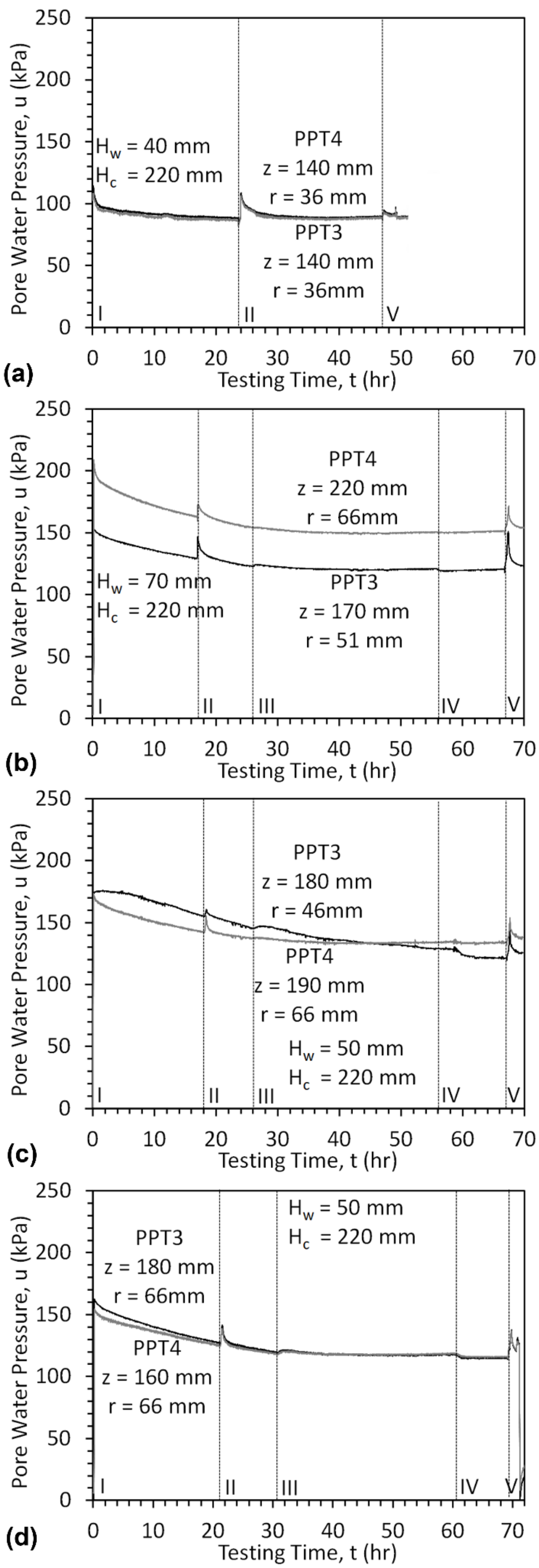

FIG. 6. Time series of pore water pressure at different radii from the torpedo pile during the five testing stages: (a) Test T1; (b) Test T2; (c) Test T3; (d) Test T4

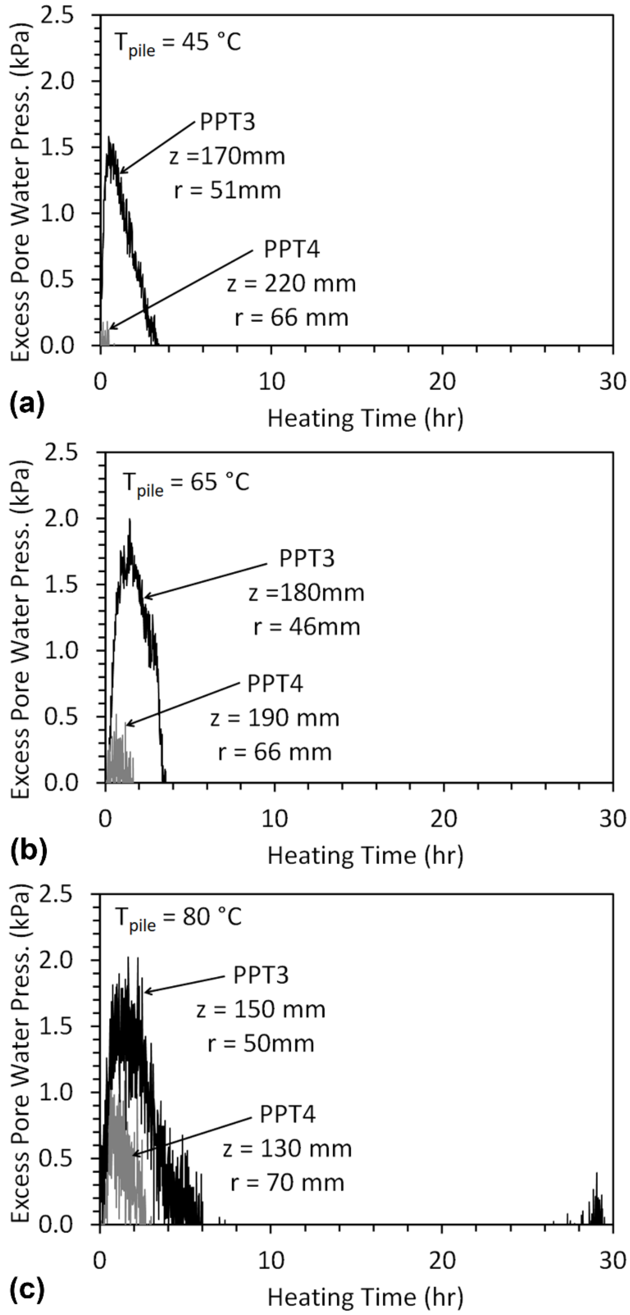

FIG. 7. Time series of excess pore water pressure at different radii from the torpedo pile during heating stage: (a) Test T1; (b) Test T2; (c) Test T3; (d) Test T4

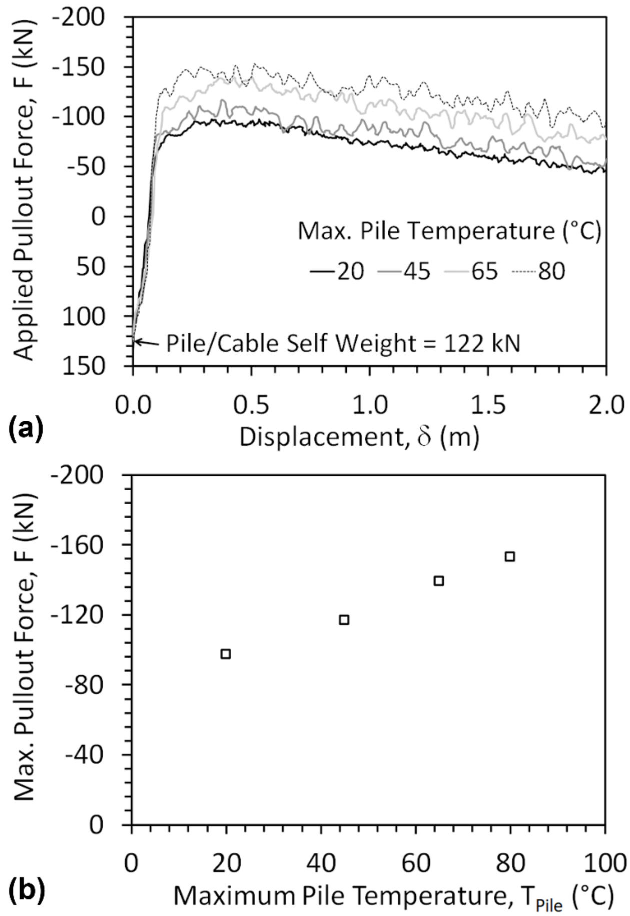

FIG. 8. Results from pullout tests on torpedo piles after a heating-cooling cycle involving different maximum pile temperatures: (a) Applied pullout force versus displacement curves (prototype scale), (b) Pullout capacity as a function of the maximum pile temperature experienced during a heating-cooling cycle

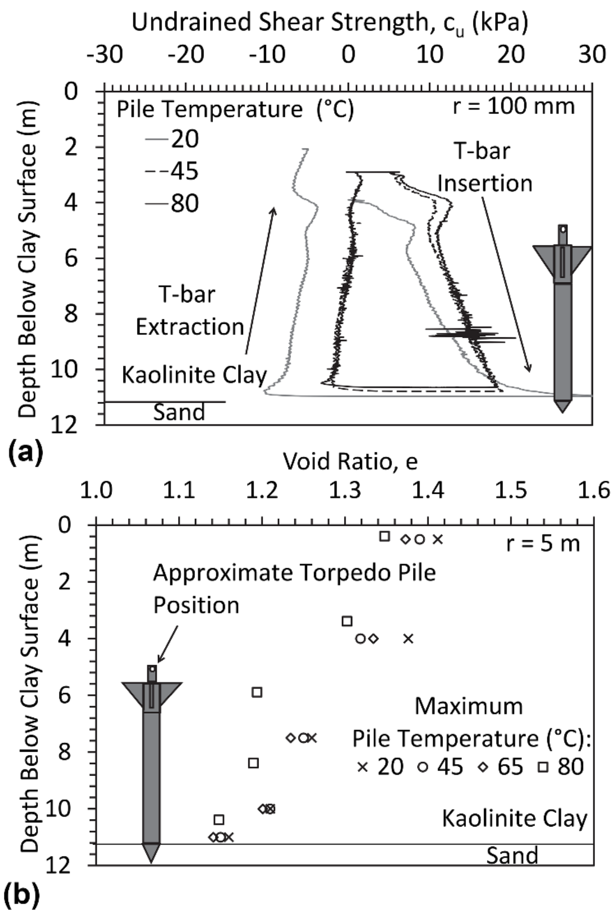

FIG. 9. (a) Prototype-scale profiles of undrained shear strength measured by the T-bar in three of the four tests on torpedo piles heated to different temperatures (positive values for insertion and negative values for extraction); (b) Prototype-scale profiles of void ratio with depth at the same radial location at the T-bar test (5 m in prototype scale or 100 mm in model scale)

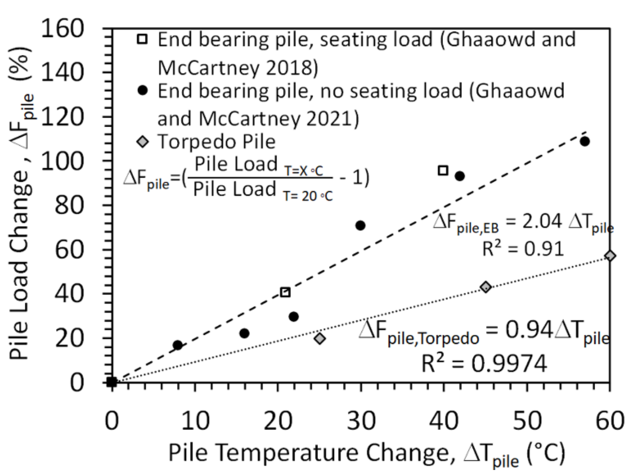

FIG. 10. Percent increase in pullout capacity of the torpedo piles in soft clay after in-situ heating to different changes in pile temperature compared with results from end bearing energy piles in soft clay